

Quantum Signatures of the Optomechanical Instability

Jiang Qian,^{1,2} A. A. Clerk,³ K. Hammerer,⁴ and Florian Marquardt^{5,6}

¹*Arnold Sommerfeld Center for Theoretical Physics,
Center for NanoScience and Department of Physics,
Ludwig-Maximilians-Universität München, Germany*

²*Department of Electrical Engineering, School of Engineering,
Case Western Reserve University, Cleveland, Ohio*

³*Department of Physics, McGill University, Montreal, Quebec, Canada H3A 2T8*

⁴*Institute for Theoretical Physics, Institute for Gravitational Physics,
Leibniz University Hanover, Callinstrasse 38, D-30167 Hanover, Germany*

⁵*Institute for Theoretical Physics, Department of Physics,
Friedrich-Alexander Universität Erlangen-Nürnberg, Staudtstr. 7, 91058 Erlangen, Germany*

⁶*Max Planck Institute for the Science of Light, Günter-Scharowsky-Straße 1/Bau 24, 91058 Erlangen, Germany*
(Dated: May 17, 2022)

In the past few years, coupling strengths between light and mechanical motion in optomechanical setups have improved by orders of magnitude. Here we show that, in the standard setup under continuous laser illumination, the steady state of the mechanical oscillator can develop a non-classical, strongly negative Wigner density if the optomechanical coupling is large at the single-photon level. Because of its robustness, such a Wigner density can be mapped using optical homodyne tomography. These features are observed near the onset of the instability towards self-induced oscillations. We show that there are also distinct signatures in the photon-photon correlation function $g^{(2)}(t)$ in that regime, including oscillations decaying on a time scale much longer than the optical cavity decay time.

By coupling optical and mechanical degrees of freedom, the emerging field of optomechanics provides exciting new opportunities to study the quantum mechanical behaviour of macroscopic objects (for reviews see [1, 2]). Recent optomechanical cooling experiments are successfully bringing nanomechanical oscillators into their quantum mechanical ground state [3, 4]. The same optomechanical coupling also promises the possibility of back-action evading quadrature measurements of the resulting mechanical quantum states with the help of the light field [5, 6]. For a reproducible and persistent quantum state, such measurements would result in an experimental determination of its full Wigner density via tomography, similar to what has been achieved in microscopic systems, for single ions or photons [7, 8]. The recent advances in fabricating optomechanical devices have drastically improved coupling parameters, e.g. for optomechanical crystals [9], in microwave setups [3], and other devices like GaAs disks [10]. It will likely be possible relatively soon to achieve optomechanical coupling strengths g_0 at the single-photon level that are comparable to the optical cavity decay rate κ , a feat that has already been achieved in cold atom optomechanical systems [11, 12]. This regime of strongly nonlinear quantum optomechanics promise to pave the way towards generating and detecting novel quantum states in optomechanical systems. It is currently only beginning to be explored theoretically [13–15], although very early work already discussed quantum optomechanical effects in the (unrealistic) absence of any dissipation [16, 17].

In the classical regime, nonlinear dynamics is known to occur when the system is driven by a blue detuned laser.

When the input laser power crosses a certain threshold, the mechanical oscillator will undergo a Hopf bifurcation and start self-induced mechanical oscillations, a mechanical analogue of lasing action [18–21]. The quantum dynamics of this regime has first been studied in [13], and there is interesting synchronization behaviour for arrays of coupled oscillators of this type [22].

In this paper, we show that, for strong optomechanical couplings, large laser driving and sufficiently low temperatures, a non-classical state of the mechanical oscillator with strongly negative Wigner density can be produced around the onset of self-induced oscillations. Because the state is time-independent, one may use back-action evading homodyne tomography to experimentally reconstruct its non-classical Wigner density.

In addition, we propose to use the two-point photon correlation function $g^{(2)}(t)$ as an experimentally convenient probe for the peculiar quantum dynamics near the bifurcation. We identify two distinct signatures that enable experimentalists to reliably detect the onset and growth of the self-induced oscillation. We provide an explanation of the non-classical decay of $g^{(2)}(t)$ in both the red and blue-detuned regime.

A standard optomechanical system can be described by the following Hamiltonian:

$$\hat{H} = \hbar(-\Delta + g_0(\hat{b}^\dagger + \hat{b}))\hat{a}^\dagger\hat{a} + \hbar\omega_M\hat{b}^\dagger\hat{b} + \hbar\alpha_L(\hat{a}^\dagger + \hat{a}) + \hat{H}_{\text{diss}}. \quad (1)$$

Here \hat{a}/\hat{b} are the operators for the photon/phonon modes, ω_M is the mechanical frequency and α_L is the laser driving amplitude. $\Delta = \omega_L - \omega_C$ is the detuning of the laser frequency from the resonant frequency of cavity at the

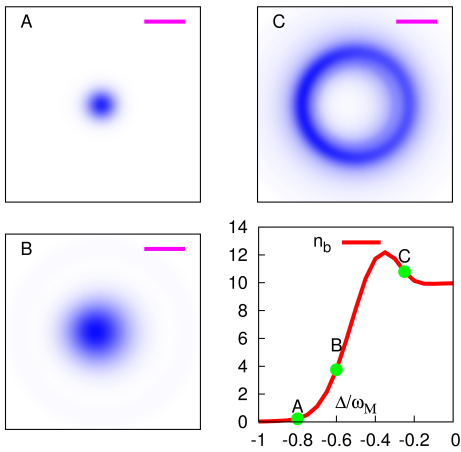


FIG. 1: The quantum self-induced oscillations in an optomechanical system. The laser power is held constant and the laser detuning Δ is being adjusted. The bottom right plot shows that, above a threshold, the phonon number n_b of the mechanical oscillator rises abruptly. The other three plots show the evolution of the mechanical Wigner density as the self-induced oscillation starts, with bars showing the reference sizes of $4x_{ZPF}$ and $4p_{ZPF}$. x_{ZPF}/p_{ZPF} are the zero-point fluctuation of the mechanical oscillator’s position/momentum. Here $g_0 = 0.36$, $\kappa = 0.3$, $\Gamma = 0.00147$, $\alpha_L = 0.311$, in units of ω_M . The photon number in the cavity is $n_a \approx 0.1 - 0.7$ when $-1 \leq \Delta \leq 0$.

mechanical displacement 0. g_0 describes the strength of the optomechanical coupling at the single-photon level.

When the dissipative terms in H_{diss} are taken into account, the density matrix $\hat{\rho}$ of the combined photon-phonon system evolves according to the quantum master equation:

$$\frac{d\hat{\rho}}{dt} = \mathcal{L}[\hat{\rho}] = \frac{[\hat{H}, \hat{\rho}]}{i\hbar} + \Gamma \mathcal{D}[\hat{b}, \hat{\rho}] + \kappa \mathcal{D}[\hat{a}, \hat{\rho}]. \quad (2)$$

Here \mathcal{L} is the quantum Liouville operator describing the time evolution of the density matrix $\hat{\rho}$, where we incorporate dissipation in the photon/phonon subsystems with decay rates κ and Γ , respectively. The standard Lindblad term is given by $\mathcal{D}[\hat{O}, \hat{\rho}] = \hat{O}\hat{\rho}\hat{O}^\dagger - \frac{1}{2}(\hat{O}^\dagger\hat{O}\hat{\rho} + \hat{\rho}\hat{O}^\dagger\hat{O})$ [30].

In this paper we are interested in the steady state solution of Eq. 2, where all the transient dynamics has died out. This is obtained numerically by finding the density matrix satisfying $\mathcal{L}[\hat{\rho}] = 0$. Due to this dynamical stability this state is thus ideal for making homodyne measurements of its mechanical Wigner density, in contrast to transient scenarios.

Specifically we are interested in the mechanical Wigner density $W_M(x, p) = \frac{1}{\pi\hbar} \int_{-\infty}^{\infty} \langle x - y | \hat{\rho}_M | x + y \rangle e^{2ipy/\hbar} dy$, where $\hat{\rho}_M$ is the mechanical density matrix, obtained by tracing out the optical degree of freedom from $\hat{\rho}$. The Wigner density is the quantum analog of the classical Liouville phase space probability density. A negative Wigner density is a strong signature of a non-classical

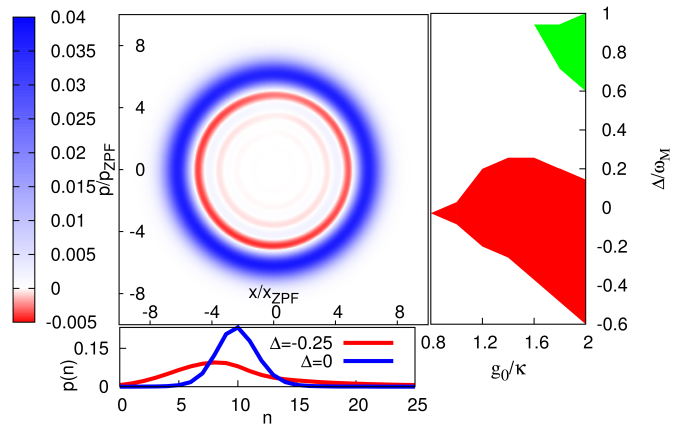


FIG. 2: *Left Top*: An example of a negative mechanical Wigner density, in this case at $\Delta = 0$. For other parameters see Fig. 1. *Left Bottom*: The negative Wigner density state $\Delta = 0$ (blue) shows narrower phonon number distribution than the near coherent state $\Delta = -0.25$ (red). *Right*: Two parameter regions where there are significant areas of negative Wigner densities. The “quantum parameter” is defined as $\zeta = g_0/\kappa$. We vary g_0 and Δ , while keeping α, κ and Γ the same as in Fig. 1.

state. Early investigations [13] of the optomechanical instability in the regime around $g_0 \sim \kappa$ had not turned up nonclassical states.

In Fig 1, we show the overall properties of the steady state solutions. As we increase the laser detuning while keeping the input laser power fixed in points $A \rightarrow B \rightarrow C$, the phonon number in the mechanical oscillator rises sharply, signaling the start of the quantum self-induced oscillation. This is also reflected in the mechanical Wigner density $W_M(x, p)$. Before the self-induced oscillation (point “A”), the oscillator stays in its ground state, with the Wigner density a simple Gaussian. The Wigner density starts to broaden just below the threshold, as the susceptibility of the system diverges and quantum fluctuations are strongly amplified (point “B”). The steady state density matrix of a periodically evolving system can be understood as the average of the Wigner density over one period, if the oscillation phase is random. In the regime of self-induced oscillations, a coherent state executes circular motion in phase space while keeping its shape, which is the picture presented at point “C”.

However, such a simple picture of a coherent state executing a semi-classical motion is inadequate for an optomechanical system with $g_0 \sim \kappa$, i.e. when one approaches the optomechanical instability deep in the quantum regime. In such a system, we observe that for a range of detuning Δ and laser driving α_L , the mechanical self-induced oscillation produces strongly non-classical states with large negative areas in the Wigner density. This can be seen in the example of Fig. 2, left panel. Negative rims develop at amplitudes slightly smaller than the

average amplitude of oscillation. The bottom left panel of Fig. 2 shows that the phonon number distribution of this state has a reduced variance (sub-Poissonian), and is thus closer to a single Fock state as compared with a coherent state [24].

The right panel of Fig. 2 maps out the regions in parameter space where negative Wigner densities occur. This ‘phase diagram’ is shown as a function of the “quantum parameter” $\frac{g_0}{\kappa}$ (see [13] for more about that parameter) and of the laser detuning Δ , at a fixed value of the laser driving strength. It has been obtained by solving for the steady state of the optomechanical system under constant illumination, and the Wigner density is considered as nonclassical if a sufficiently large area turns out to be negative [31]. The numerical results shown here indicate that, starting at a “quantum parameter” $\frac{g_0}{\kappa} = 0.8$, the negative Wigner density states appear around detuning $\Delta = 0$, and a second negative Wigner density region opens up at $\frac{g_0}{\kappa} = 1.6$, around $\Delta/\omega_M = 0.9$ at the first blue sideband, where the instability is driven efficiently. The phonon number distribution displays a pronounced narrowing, getting closer to a single mechanical Fock state. However, we find that still many photon/phonon levels are involved in the dynamics in the regime considered here, and there seems to be no simple explanation starting from a discrete energy level scheme.

These *steady-state* non-classical Wigner densities could be reconstructed via optomechanical QND quadrature detection [5] and subsequent quantum state tomography [26]. This merely involves illumination with another amplitude-modulated laser beam for read-out, as explained in [5]. When observed, these would provide an accessible example of non-classical states in a fabricated mesoscopic mechanical object. To date, there has been no experimental observation of non-classical Wigner densities in the domain of micro- or nanomechanical structures. The experiment that came closest to that goal, and in the process did produce nonclassical mechanical Fock states, employed a complex multi-layered superconducting circuit with piezoelectric coupling to a superconducting qubit and ultrafast pulse sequences [27]. Furthermore in their setup the resonator lifetime is too short to permit the reconstruction of the full Wigner density. By contrast, once optomechanical parameters can be improved to reach the single-photon strong coupling regime, the scheme discussed here would be relatively straightforward, being based on continuous laser illumination of an optomechanical setup whose fabrication is much less complex as it involves only one material. And the non-classical states obtained are long-living and amicable to quantum homodyne Wigner density reconstruction. In addition, there is the possibility that the parameters required here may be reached in cold atom optomechanical setups [11, 12].

The full reconstruction of the mechanical Wigner density of an optomechanical system in the nonlinear quan-

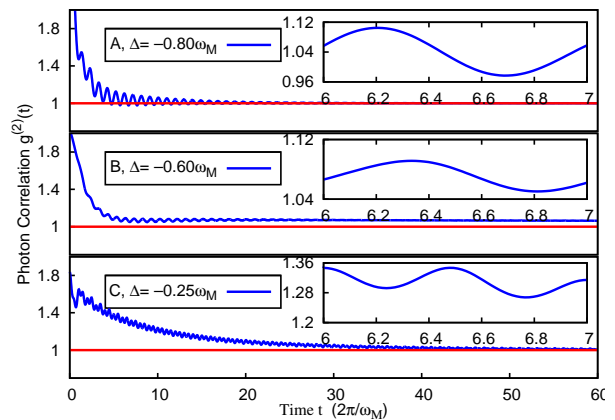


FIG. 3: Time-dependence of photon-photon correlations near the regime of quantum optomechanical oscillations. “A,B,C” labels the same parameters as in Fig. 1. Apart from observing photon bunching and oscillations of the correlation function at the mechanical period, these plots show that there is a remarkably slow long-term decay near the onset of self-induced oscillations, *e.g.* at point “B” (see main text). The insets show that the fully developed oscillation beyond the threshold, at point “C”, leads to higher harmonics.

tum regime is obviously an enticing and challenging goal. Nevertheless, it requires repeated measurements of many identically prepared quantum states. It will be helpful to have other means of optically probing the quantum dynamics of the system near the relevant regime around the onset of the instability. When the system itself is in a steady state, the expectation values of physical observables do not change in time. A suitable probe for the dynamics is then provided by the photon two-point correlation function:

$$g^{(2)}(t) = \frac{\langle a_{\tau}^{\dagger} a_{\tau+t}^{\dagger} a_{\tau+t} a_{\tau} \rangle}{(\langle a_{\tau}^{\dagger} a_{\tau} \rangle)^2}. \quad (3)$$

The $\langle \dots \rangle$ denotes the statistical average over $\hat{\rho}$ in Eq. 2. In steady state, $g^{(2)}$ does not depend on the initial time τ . Photon correlations are readily accessible in nowadays quantum optics experiments with single-photon detectors (*e.g.* using a Hanbury-Brown Twiss setup), and they have been successfully employed to characterize the change of photonic statistics upon transmission through nonlinear systems. The most important example is photon anti-bunching in the resonance fluorescence of single photon emitters, which has recently also been predicted to occur in optomechanical systems for sufficiently strong coupling [14].

As can be seen in Fig. 3, there are clear signatures in the photon correlations when the quantum self-induced oscillations start (around point “B”).

In particular, $g^{(2)}(t)$ persists at some value above unity over a very long time (middle panel, Fig. 3). It can be proven that as long as the steady state of the system is not degenerate, we always have $g^{(2)}(t) \rightarrow 1 +$

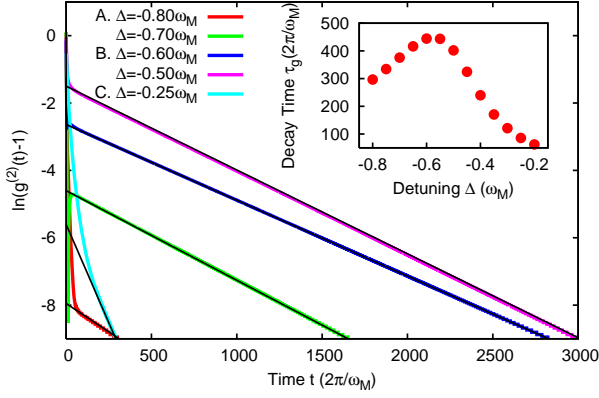


FIG. 4: Quantifying the slow approach of $g^{(2)}(t) \rightarrow 1$ near the onset of the quantum self-induced oscillations, as observed in Fig. 3. $g^{(2)}(t) - 1$ obeys an exponential decay e^{-t/τ_g} in the long-time limit $t \rightarrow \infty$. The inset shows the decay time τ_g peaking toward very large values around point B, *i.e.* $\Delta = 0.6\omega_M$.

$\alpha \exp(-t/\tau_g)$ in the long-time limit $t \rightarrow \infty$. Here the decay rate $1/\tau_g = \text{Re}(\lambda_1)$, where λ_1 is the eigenvalue of the Liouville operator \mathcal{L} in Eq. 2 with the largest non-zero real part, characterizing the slowest decay in the system. This signature can be examined by plotting $\ln(g^{(2)}(t) - 1)$ to extract τ_g , which indeed agrees with the λ_1 obtained numerically from \mathcal{L} (see Fig. 4). As can be seen in the inset, τ_g rises strongly around the start of the quantum self-induced oscillation (point B), resulting in a long-term persistence of $g^{(2)}(t)$ above 1 (although it finally decays to 1). This is connected to the fact that classically the overall mechanical damping rate goes to zero near the Hopf bifurcation [19].

The second signature in $g^{(2)}$ is the appearance of higher harmonics when the quantum self-induced oscillation is fully developed (see insets of Fig. 3). Both the long-term decay of $g^{(2)}(t)$ and the higher harmonics appearing above the bifurcation threshold can best be understood in a semiclassical picture. To this end, we approximate the photon correlator via the classical intensity correlator, $\langle |\alpha(t+\tau)|^2 |\alpha(\tau)|^2 \rangle_\tau$. The light amplitude $\alpha(t) = e^{i\phi(t)} \sum_n \alpha_n e^{in\omega_M t}$ is modulated harmonically by the mechanical oscillations, as detailed in [19]. However, to obtain the *decay* of the resulting oscillations in the correlator, we have to take into account the mechanical phase diffusion induced by the radiation pressure shot noise. This was considered in [28], but here we discuss another, quite straightforward analytical approach:

$$\delta\phi(t) = \frac{1}{m\omega_M A} \int_0^t dt' F(t') \cos(\phi(t')), \quad (4)$$

$$\text{Var}(\delta\phi(t)) = \frac{1}{(m\omega_M A)^2} \frac{t}{4} (S_{FF}(\omega_M) + S_{FF}(-\omega_M)).$$

Here S_{FF} is the force noise spectrum (see [29]). We

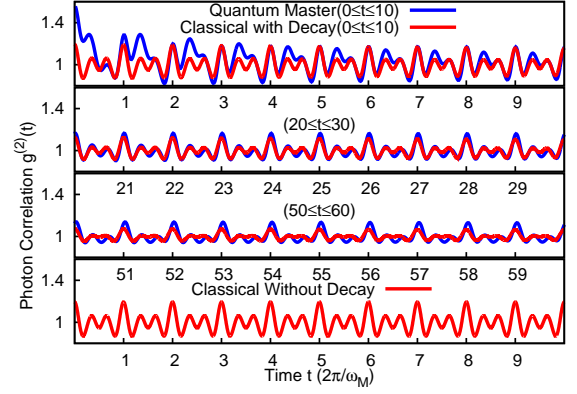


FIG. 5: Semiclassical approximation for photon correlations in the mechanical lasing regime of optomechanics. By adding the mechanical phase-diffusion to the classical light field dynamics (red), one can qualitatively account for the slow long-time decay of the photon correlator $g^{(2)}(t)$ in the full quantum simulation (blue). The lowest panel compares the classical solution without phase diffusion (here $\Delta = \omega_M$).

find

$$\begin{aligned} \langle |\alpha(t+\tau)|^2 |\alpha(\tau)|^2 \rangle_\tau &= \sum_{n=-\infty}^{\infty} Z_n e^{in\omega_M t} \langle e^{in(\delta\phi(t+\tau) - \delta\phi(t))} \rangle \\ &= Z_0 + 2 \sum_{n=1}^{\infty} Z_n \cos(n\omega_M t) e^{-\frac{n^2}{2} \text{Var}(\delta\phi(t))}, \end{aligned}$$

where $Z_n = |\sum_{m=-\infty}^{\infty} \alpha_m \alpha_{m-n}^*|^2$ (for more details see the supplementary material). This theory explains at least qualitatively the shape of the correlator even deep in the quantum regime (see Fig. 5).

Finally, we can also quantify the decay of $g^{(2)}(t)$ in the red detuned regime, before the start of the self-induced oscillation. Semiclassically, there is no mechanical motion in this regime, and thus the dynamics $g^{(2)}(t)$ cannot be explained. But we have found that the correlator decay is then well described by the optomechanical cooling rate (see supplementary materials).

To summarize, in this paper we investigated quantum signatures of light and mechanics for an optomechanical system in the “mechanical lasing” regime. We found that, for strong optomechanical coupling ($g_0 \sim \kappa$), for a range of detuning and input power the steady state mechanical Wigner density contains strong negative parts, signaling stable non-classical states. Back-action evading homodyne measurements can be used to reconstruct these Wigner densities. In addition, the two-point photon correlator $g^{(2)}(t)$ displays clear signatures near the onset of oscillations. Finally we explained the slow long-time decay of the photon correlations as being due to the mechanical phase diffusion induced by photon shot noise. One should note that experimental observation of some

of these photon correlation features does not necessarily require being in the nonlinear quantum regime and could actually succeed even in present setups.

F.M. acknowledges the DFG (Emmy-Noether) and an ERC Starting Grant. F.M. and A.C. acknowledge the DARPA ORCHID program. J.Q. acknowledges the support of DPG SBF 631 Grant. K.H acknowledges the support through QUEST.

[1] F. Marquardt and S. M. Girvin, *Physics* **2**, 40 (2009)
[2] T. J. Kippenberg and K. J. Vahala, *Science* **321**, 1172 (2008)
[3] J. D. Teufel *et al.*, *Nature* **475**, 359 (2011)
[4] J. Chan, T. P. M. Alegre, A. H. Safavi-Naeini, J. T. Hill, A. Krause, S. Groblacher, M. Aspelmeyer, and O. Painter, *Nature* **478**, 89 (2011)
[5] A. A. Clerk, F. Marquardt, and K. Jacobs, *New Journal of Physics* **10**, 095010 (2008)
[6] J. B. Hertzberg, T. Rocheleau, T. Ndukum, M. Savva, A. A. Clerk, and K. C. Schwab, *Nature Physics* **6**, 213 (2010)
[7] D. Leibfried, D. M. Meekhof, B. E. King, C. Monroe, W. M. Itano, and D. J. Wineland, *Phys. Rev. Lett.* **77**, 4281 (1996)
[8] A. I. Lvovsky, H. Hansen, T. Aichele, O. Benson, J. Mlynek, and S. Schiller, *Phys. Rev. Lett.* **87**, 050402 (2001)
[9] M. Eichenfield, J. Chan, R. M. Camacho, K. J. Vahala, and O. Painter, *Nature* **462**, 78 (2009)
[10] L. Ding *et al.*, *Phys. Rev. Lett.* **105**, 263903 (2010)
[11] K. W. Murch, K. L. Moore, S. Gupta, and D. M. Stamper-Kurn, *Nature Physics* **4**, 561 (2008)
[12] F. Brennecke, S. Ritter, T. Donner, and T. Esslinger, *Science* **322**, 235 (2008)
[13] M. Ludwig, B. Kubala, and F. Marquardt, *New Journal of Physics* **10**, 095013 (2008)
[14] P. Rabl, *Phys. Rev. Lett.* **107**, 063601 (2011)
[15] A. Nunnenkamp, K. Børkje, and S. M. Girvin, *Phys. Rev. Lett.* **107**, 063602 (2011)
[16] S. Mancini, V. I. Man'ko, and P. Tombesi, *Phys. Rev. A* **55**, 3042 (1997)
[17] S. Bose, K. Jacobs, and P. L. Knight, *Phys. Rev. A* **56**, 4175 (1997)
[18] T. Carmon, H. Rokhsari, L. Yang, T. Kippenberg, and K. Vahala, *Phys. Rev. Lett.* **94**, 223902 (2005)
[19] F. Marquardt, J. G. E. Harris, and S. M. Girvin, *Phys. Rev. Lett.* **96**, 103901 (2006)
[20] C. Metzger, M. Ludwig, C. Neuenhahn, A. Ortlieb, I. Favero, K. Karrai, and F. Marquardt, *Physical review Letters* **101**, 133903 (2008)
[21] I. S. Grudin, H. Lee, O. Painter, and K. J. Vahala, *Physical Review Letters* **104**, 083901 (2010)
[22] G. Heinrich, M. Ludwig, J. Qian, B. Kubala, and F. Marquardt, *Phys. Rev. Lett.* **107**, 043603 (2011)
[23] Note that we have assumed zero bath temperature in our simulations, which will be reachable to a good approximation when GHz-frequency setups (such as optomechanical crystals) are employed in dilution refrigerator settings.

[24] D. A. Rodrigues and A. D. Armour, *Phys. Rev. Lett.* **104**, 053601 (2010)
[25] To rule out cases with negligible negative content that would be hard to measure and may be subject to numerical errors, we choose the threshold to be that the negative area is at least 5% of the positive area, clearly legible on the plotted Wigner density and the minimum in Wigner density is at least 5% in absolute value of the maximum.
[26] A. I. Lvovsky and M. G. Raymer, *Reviews of Modern Physics* **81**, 299 (2009)
[27] A. D. O'Connell, M. Hofheinz, M. Ansmann, R. C. Bialczak, M. Lenander, E. Lucero, M. Neeley, D. Sank, H. Wang, M. Weides, J. Wenner, J. M. Martinis, and A. N. Cleland, *Nature* **464**, 697 (2010)
[28] K. J. Vahala, *Phys. Rev. A* **78**, 023832 (2008)
[29] F. Marquardt, J. P. Chen, A. A. Clerk, and S. M. Girvin, *Phys. Rev. Lett.* **99**, 093902 (2007)
[30] Note that we have assumed zero bath temperature in our simulations, which will be reachable to a good approximation when GHz-frequency setups (such as optomechanical crystals) are employed in dilution refrigerator settings.
[31] To rule out cases with negligible negative content that would be hard to measure and may be subject to numerical errors, we choose the threshold to be that the negative area is at least 5% of the positive area, clearly legible on the plotted Wigner density and the minimum in Wigner density is at least 5% in absolute value of the maximum.

Appendices

Under the experimentally realistic assumptions, when the classical self-induced oscillation starts, it is to a good approximation harmonic $x(t) \approx \bar{x} + A \cos(\omega_M t)$. The laser amplitude, influenced by the mechanical oscillation, will contain higher harmonics [19] $\alpha(t) = e^{i\phi(t)} \sum_n \alpha_n e^{in\omega_M t}$, where

$$\alpha_n = \frac{\alpha_L J_n(-g_0 A)}{-n\omega_M + (\Delta + g_0 \bar{x}) + i\kappa/2} \quad (\text{A-5})$$

and $\phi(t) = g_0 A \sin(\omega_M t)$. Here we take the length unit to be the mechanical zero point fluctuation x_{ZPF} and frequency unit to be ω_M . $J_n(x)$ is the n-th order Bessel function. The oscillation amplitude A and equilibrium position \bar{x} can be determined self-consistently. We can express $g^{(2)}(t)$ in terms of the solution in Eq. A-5:

$$Z_n = \left| \sum_{m=-\infty}^{\infty} \alpha_m \alpha_{m-n}^* \right|^2, \quad \langle |\alpha(\tau)|^2 \rangle_\tau = \sum_{n=-\infty}^{\infty} |\alpha_n|^2 = Z_0.$$

$$\langle |\alpha(t+\tau)|^2 |\alpha(\tau)|^2 \rangle_\tau = Z_0 + 2 \sum_{n=1}^{\infty} \cos(n\omega_M t) Z_n. \quad (\text{A-6})$$

In this paper we're interested in the strongly quantum regime where $g_M \approx \kappa$, thus in the sideband resolved regime we have $g_M/\omega_M < 1$. From Eq. A-5 we see that

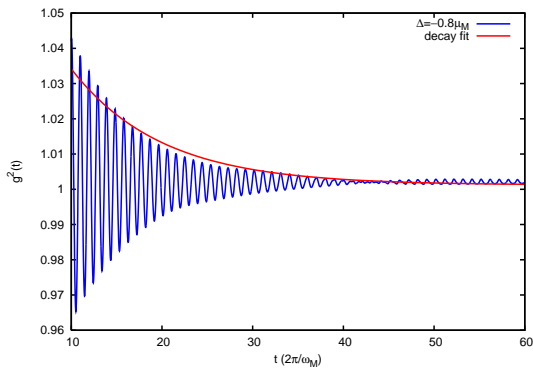


FIG. 6: The decay of the correlation function $g^{(2)}(t)$ in the red-detuned regime $\Delta = -0.8\omega_M$ can be qualitatively accounted for with Γ_{opt} obtained from optomechanical cooling.

only when $A \gg x_{ZPF}$ would there be significant contribution of higher harmonics in the light amplitude $\alpha(t)$, which, as can be seen from Eq. A-6 is also the condition of having higher harmonics in $g^{(2)}(t)$. This explains qualitatively the appearance of higher harmonics when the quantum self-induced oscillation gains large amplitude.

However, even when the self-induced oscillation has amplitude much larger than the x_{ZPF} , there are important quantum effects that are not accounted for by Eq. A-5 and Eq. A-6. As seen in Fig. 5, the classical solution (bottom) is fully periodic, as there is a balance between the optical and mechanical dissipation and laser driving. However, over the period of 60 cycles, the amplitude of the quantum mechanical $g^{(2)}(t)$ decays significantly (top three panels, blue curves). We can qualitatively account for this decay by calculating the influence of photon shot noise on the phase fluctuation of the mechanical oscillator.

Because of the optomechanical coupling in Eq. 1, the photon shot noise influences the phase of the mechanical oscillation through radiation pressure $F(t) = (\hbar\omega_R/L)a(t)^\dagger a(t)$:

$$\delta\phi(t) = \frac{1}{m\omega_M A} \int_0^t dt' F(t') \cos(\phi(t')), \quad (\text{A-7})$$

$$\text{Var}(\delta\phi(t)) = \frac{1}{(m\omega_M A)^2} \frac{t}{4} (S_{FF}(\omega_M) + S_{FF}(-\omega_M)).$$

The noise spectrum of the radiation force is can be easily computed [19]:

$$S_{FF}(\omega) = \left(\frac{\hbar\omega_R}{L}\right) \bar{n}_p \frac{\kappa}{(\omega + \Delta)^2 + (\kappa/2)^2}. \quad (\text{A-8})$$

The fluctuations of the mechanical oscillator's phase feed back to the time-dependence of optical amplitude. Thus, under the semi-classical assumption where we take into account the photon shot noise but still treat the photon amplitude classically, we can modify Eq. A-6 to be:

$$\begin{aligned} \langle |\alpha(t+\tau)|^2 |\alpha(\tau)|^2 \rangle_\tau &= \sum_{n=-\infty}^{\infty} Z_n e^{in\omega_M t} \langle e^{in(\delta\phi(t+\tau) - \delta\phi(t))} \rangle \\ &= Z_0 + 2 \sum_{n=1}^{\infty} Z_n \cos(n\omega_M t) e^{-\frac{n^2}{2} \text{Var}(\delta\phi(t))}. \end{aligned}$$

Here we assume the phase fluctuation $\delta\phi$ is Gaussian. The result of this semi-classical accounting of the photon shot noise can be seen in the red curves in the top three panels of Fig. 5. We can see that this simple analysis can account qualitatively for the decay of the $g^{(2)}(t)$ in the large amplitude self-induced oscillation regime.

Finally, as we see in Fig. 6, there are also significant oscillation structure and decay for the $g^{(2)}(t)$ in the so-called red detuned regime, before the start of the self-induced oscillation. This regime cannot be understood at all by the classical picture, since classically the system has no dynamics there. The oscillation in $g^{(2)}(t)$ can be understood as the dynamical response of the mechanical oscillator to the quantum fluctuation of the photon field. The decay can then be modeled using the theory of the optomechanical cooling of the mechanical oscillation in the red detuned regime, giving a cooling rate

$$\Gamma_{opt} = \frac{x_{ZPF}^2}{\hbar^2} [S_{FF}(\omega_M) - S_{FF}(-\omega_M)]. \quad (\text{A-9})$$

Here S_{FF} is the same noise spectrum given by Eq. A-8. As seen in Fig. 6, this rate gives a qualitative account for the decay rate of $g^{(2)}(t)$ in the red-detuned regime.